Review Article

Development of a gamma irradiation loop to evaluate the performance of a EURO-GANEX process

I. Sánchez-García [a, b, *], H. Galán [a, *], A. Núñez [a], J.M. Perlado [b], J. Cobos [a, c]

[a] Centro de Investigaciones Energéticas, Medioambientales y Tecnológicas (CIEMAT), Avda. Complutense 40, 28040, Madrid, Spain
[b] Universidad Politécnica de Madrid (UPM), Instituto de Fusión Nuclear, C/ José Gutiérrez Abascal 2, 28006, Madrid, Spain
[c] Estación Biológica de Doñana (EBD-CSIC), Avda. Américo Vespucio 26, 41092, Sevilla, Spain

ABSTRACT

A new irradiation loop design has been developed, which provides the ability to carry out radiolytic resistance studies of extraction systems simulating process relevant conditions in an easy and simple way. The step-by-step loop configuration permits an easy modification of settings and has a relative low volume requirement. This irradiation loop has been initially set up to test the main EURO-GANEX process steps: the lanthanide (Ln) and actinide (An) co-extraction followed by the transuranic (TRU) stripping. The performance and changes in the composition have been analyzed during the irradiation experiment by different techniques: gamma spectroscopy and ICP-MS for the extraction and corrosion behavior of the full system, and HPLC-MS and Raman spectroscopy to determine the degradation of the organic and aqueous solvents, respectively. The Ln and An co-extraction step and the corrosion that occurred during the first irradiation step revealed the favorable expected results according to literature. The effects of acidity changes occurred during the irradiation process, the presence of stainless corrosion products in solution as well as the new possible degradation compounds have been explored in the An stripping step. The results obtained demonstrate the importance of developing realistic irradiation experiments where different factors affecting the performance can be easily studied and isolated.

© 2021 Korean Nuclear Society, Published by Elsevier Korea LLC. This is an open access article under the CC BY-NC-ND license (http://creativecommons.org/licenses/by-nc-nd/4.0/).

1. Introduction

The reprocessing of nuclear fuel is moving towards advanced cycles that include the recycling of Minor Actinides (MAs: Np-Cm) as a strategy to minimize the radiotoxicity of the waste generated [1–4]. Therefore, new solvent extraction-based separation processes for actinides (An) and fission products (FP) reprocessing are under development globally [5–9]. To validate a new separation process for this purpose, solvents are not only tested concerning the extraction efficiency but also their resistance to radiolysis and hydrolysis. This is because extraction systems will be in contact with a highly radioactive field and high nitric acid concentration, inducing its degradation and further undesirables effects such as loss of selectivity, settling issues, etc., and the consequent increase

of secondary waste and process costs. Degradation Compounds (DCs) are one of the biggest barriers to advanced reprocessing solvents since they are progressively formed and could have different properties from those of the original system [10,11]. Hence, the development of a successful industrial process demands an ability to understand and quantify stability issues, from the initial design of the extractant to a hot test in a pilot plant. The initial irradiation studies of individual solvents with isolated molecules in batch and static conditions allow the fundamental comprehension of the degradation pathways and are an easy way to compare the robustness of different extractants. However, it is also known that the variation of experimental conditions during the irradiation process, like presence of oxygen, solvent compositions, phases contacted, etc., can give rise to different results [12–14]. Consequently, to predict and anticipate the long-term behavior during operations, a more realistic assessment of the process conditions must be considered. Although batch irradiation experiments can be designed to cover many options, dynamic experiments, as lifelike as possible, are necessary. It is clear that there is an important gap between fundamental irradiation experiments and advanced tests in pilot plants, which require sophisticated

* Corresponding authors. Centro de Investigaciones Energéticas, Medioambientales y Tecnológicas (CIEMAT), Avda. Complutense 40, 28040, Madrid, Spain.
E-mail addresses: ivan.sanchez@ciemat.es (I. Sánchez-García), hitos.galan@ciemat.es (H. Galán).

I. Sánchez-García, H. Galán, A. Núñez et al.

dynamic irradiation platforms (irradiation loops) where the settings are often not easily modified. CEA Marcel-Proust loop (Commissariat à l'énergie atomique et aux énergies alternatives) in France [15] and the Idaho National Laboratory (INL) loop in the United States [16] are two of the most successful irradiation loops developed, until now. Different extraction processes like DIAMEX (*DIAMide EXtraction*), GANEX (*Grouped ActiNides EXtraction*) first cycle [17], *i*-SANEX (*Innovative Selective ActiNide EXtraction*) [18] or ALSEP (*Actinides and Lanthanides SEParation*) [19] have been tested using these loops.

In this work, an irradiation test loop has been developed in the Náyade facility at CIEMAT, which provides the possibility to perform easily modifiable dynamic irradiation experiments where conditions relevant to the advanced reprocessing processes can be studied. Moreover, this design allows the irradiation of two phases in contact, its configuration step-by-step improves the simulation of the doses expected for each phase, but also permits a straightforward modification of experiment settings and has a low solvent volume requirement.

The new irradiation loop has been adapted to assess the performance of the EURO-GANEX process [20–22], taking as a starting point our previous studies regarding the development of experimental irradiation strategies to evaluate the robustness of extraction systems involved in different processes [23,24].

As part of a homogeneous actinides recycling strategy [2,5], the GANEX concept consists of two cycles: the first one for the bulk recovery of uranium (U) and the second one aims to separate the transuranic elements (TRU) together [25]. The EURO-GANEX process is one of the most promising options for GANEX second cycle, based on the complementary selectivity of extractants used in the organic and complexing agents employed in the aqueous phase [20], which comprises two steps, the co-extraction of An and Ln and the TRU stripping [22]. In the An and Ln co-extraction, a solvent consisting of TODGA (*N,N,N′,N′*-tetraoctyl diglycolamide [26,27], Fig. 1) and DMDOHEMA (*N,N′*-dimethyl-*N,N′*-dioctylhexylethoxymalonamide [28], Fig. 1) in Exxsol D80 (a kerosene diluent) is mixed with a feed, which is the GANEX first cycle raffinate and CDTA (*trans*-1,2-cyclohexanediaminetetraacetic acid, Fig. 1), which prevents the co-extraction of Pd(II) and Zr(IV) [29]. The role of DMDOHEMA in the EURO-GANEX solvent is to prevent third phase formation and increase the Pu loading capacity of the organic phase [22]. After the co-extraction step, a scrubbing step is required to

remove the co-extracted elements such as Sr, Fe, Mo, Ru and Tc, among others [22]. Then, the TRU elements are selectively recovered into the aqueous phase in the TRU stripping step using a combination of two water-soluble complexants in a lower nitric acid concentration: a sulphonated bis-triazinyl pyridine (2,6-bis(5,6-di-(sulfophenyl)-1,2,4-triazin-3-yl)-pyridine (SO$_3$-Ph-BTP) [30] and acetohydroxamic acid (AHA) [31], both in Fig. 1. SO$_3$-Ph-BTP is used to strip Am(III) and Cm(III) selectively from Ln [30], while AHA is added to strip Pu(IV), Np(IV), and Np(VI) [22,31–33].

It is known that TODGA-based solvents show moderate resistance to radiation, approximately reducing by half its concentration after 500 kGy and forming a series of DCs that alter the extraction properties [10,34–36]. However, the stability studies regarding the stripping aqueous phase containing the SO$_3$-Ph-BTP are less conclusive since its resistance to radiation is highly affected by the experimental conditions studied [37,38]. We have recently published on the topic of design strategies to study the stability of TODGA/SO$_3$-Ph-BTP systems, explaining the reasons for some of these different results [23]. In the present work, the challenge is to extend these strategies to dynamic experiments using a new loop design.

Based on all previous studies [23,24,37,38], to simulate the most relevant aspects of these processes, the design of the loop should involve the irradiation of two phases in contact and take into account its composition, the nitric acid concentration, the renewal of oxygen content and the dose expected for each phase. With this purpose, phases will be mixed under an open air atmosphere outside the irradiator device and irradiated together when they pass through the irradiator coil. Considering that the organic phase will be recycled as much as possible, it will be submitted to high doses; however, at present, it is not anticipated that the aqueous phase will be recycled [22]. Therefore, the loop experiment was divided into three steps (Fig. 2). The first, where the organic phase will be irradiated in contact with a high nitric acid concentration solution to high doses (500 kGy) to simulate the behavior after many An + Ln co-extraction cycles, where all possible TODGA and DMDOHEMA DCs can be identified, allowing a direct comparison with previous stability studies of TODGA/SO$_3$-PhBTP systems [23,24]. A second, to carry out the corresponding scrubbing step at a lower nitric acid concentration, which mimics the removal of other elements such as co-extracted FP and adjusts the acidity for the next step. And the last step, where the previously degraded and
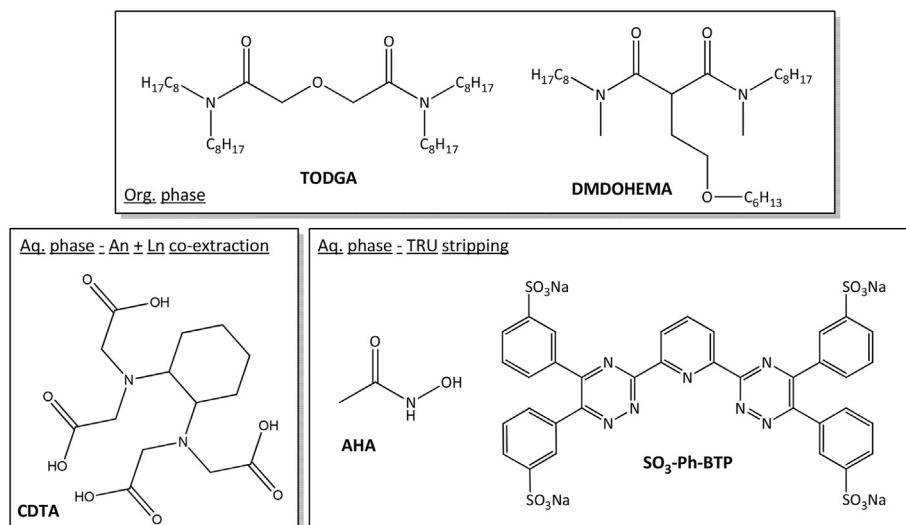

Fig. 1. Structures of the molecules involved in the EURO-GANEX process: TODGA and DMDOHEMA in the organic phase and CDTA in the aqueous phase during An + Ln co-extraction; and the same organic phase and AHA and SO$_3$-Ph-BTP in the aqueous phase for TRU stripping step.
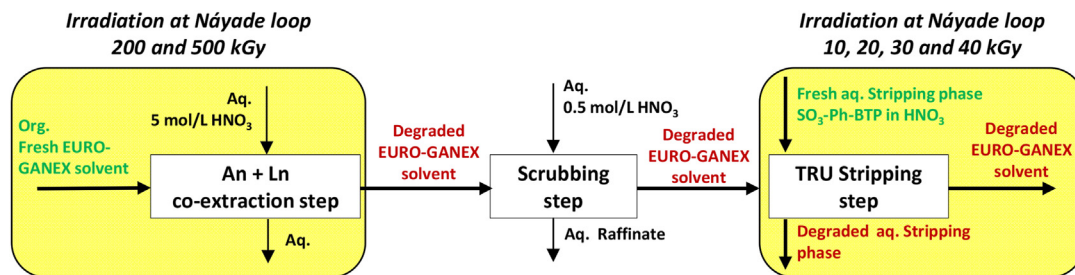
Fig. 2. Scheme of the main steps of EURO-GANEX process simulated at Náyade irradiation test loop.

scrubbed organic phase is irradiated again in contact with the stripping aqueous phase to a relatively low dose (40 kGy), to simulate the TRU stripping step. During the first irradiation step, CDTA was not included because the dose applied (500 kGy) is much higher compared to that expected for CDTA in each single pass aqueous phase. AHA has not been included in loop irradiation experiments either due to the long irradiation times needed to perform irradiation experiment compared to its hydrolysis rate as it would have undergone complete hydrolysis during the irradiation, and its effects over the Ln extraction efficiency observed in our previous works [39].

After irradiation, the extraction behavior has been analyzed by gamma spectroscopy, for ^{241}Am and ^{152}Eu, and inductively coupled plasma-mass spectrometry (ICP-MS) for the non-active elements present in a simulated High Active Raffinate (HAR) solution; in addition, the composition was evaluated by high-pressure liquid chromatography-mass spectrometry (HPLC-MS) for the organic phases and by Raman spectroscopy specifically for SO$_3$-Ph-BTP in the aqueous phase.

2. Experimental section

2.1. Materials

The extractants used in the organic phase were *N,N,N′,N′*-tetraoctyldiglycolamide (TODGA) and *N,N′*-dimethyl-*N,N′*-dioctylhexylethoxymalonamide (DMDOHEMA). TODGA was synthesized at CIEMAT, modifying an existing literature procedure under air and without dried solvent [40]. The raw product was then purified by column chromatography (silica gel, 98:2 %$_{vol}$ CH$_2$Cl$_2$/MeOH) to give TODGA as an oil. The purity of the compound, as determined by HPLC-MS, was 98%. DMDOHEMA with a purity of 99% by HPLC-MS was purchased from Technocomm Ltd (United Kingdom). The diluent used in the organic phase was odourless kerosene (OK) and it was purchased from Alfa Aesar (Germany).

The reagents in the aqueous phase were the water-soluble BTP (2,6-bis(5,6-di-(sulfophenyl)-1,2,4-triazin-3-yl)-pyridine, SO$_3$-Ph-BTP) and the masking agent *trans*-1,2-cyclohexanediaminetetraacetic acid (CDTA). SO$_3$-Ph-BTP with a purity of 98% by HPLC-MS and CDTA with a purity of 98.5% were purchased from Technocomm Ltd (United Kingdom) and Sigma-Aldrich (Germany), respectively. These reagents were used without further purification. Nitric acid used was purchased from VWR Chemical as nitric acid (HNO$_3$) 65% with the grade AnalaR NORMAPUR for analysis; it was additionally purified twice by a Quartz sub-boiling distillation system (MLS-Milestone) and used in a short period of time. The HNO$_3$ solutions were prepared by diluting concentrated nitric acid with ultrapure water (18 MΩ/cm). The radioactive tracer solutions of ^{241}Am(III) and ^{152}Eu(III), were obtained as MCl$_3$, in HCl 1 mol/L, from Isotope Products Laboratories, California (US). Highly Active Raffinate (HAR) solution was

used to simulate the high-level waste stream after reprocessing typical spent fuels. It was prepared by a specific strategy for the dissolution of the reagents, which is mainly based on the use of metal nitrate salts [36]. The composition is described in the solvent extraction performance section.

2.2. Irradiation test loop

Irradiation experiments of the extraction systems involved in the different steps of the loop were performed at the Náyade facility (CIEMAT) [41]. It consists of a pool of a 1.2 m^2 by 4.5 m deep that uses water as the biological shield. At the bottom of the pool, there are 60 sources of ^{60}Co (15 mm diam. x 135 mm long each) with a total activity of 3.22·10^{14} Bq. The cylindrical irradiation container used receives a homogeneous irradiation flux within a 60 mm diam. x 100 mm high.

Solvents to be irradiated are mixed outside of the pool, at a 1:1 volume ratio and open air atmosphere, pumped by peristaltic pumps through a 316 stainless steel coil designed and manufactured at CIEMAT (10 mm outside and 8 mm inner diameters and 110 mm length) for the irradiation (Fig. 3). Stainless steel has been selected as the centrifugal contactors that are planned for use in advanced reprocessing are also made of this material [42]. The main elements in the composition of the 316 stainless steel material are Fe, Cr, Ni and Mo, and they should be taken into account as corrosion products when this material is exposed to extreme conditions such as concentrated acid solutions and radiation fields. The stainless steel coil was introduced in the hermetic irradiation
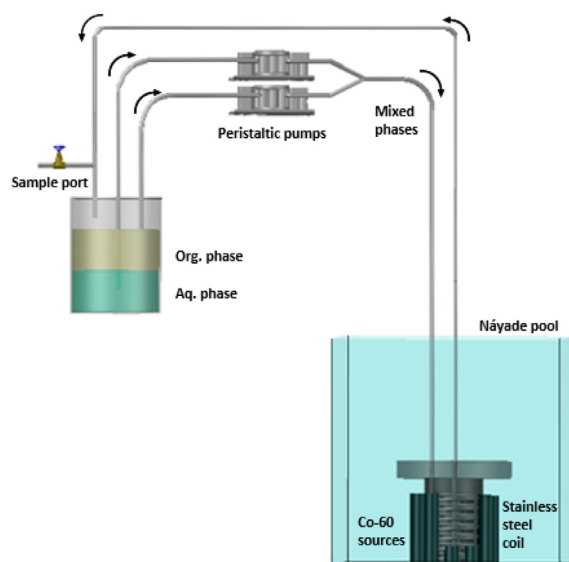

Fig. 3. Schematic diagram of the irradiation test loop.

device located at the bottom of the pool, which has also been designed and manufactured at CIEMAT with special entrances for tubing, whilst preventing water ingress. The ISO-VERSINIC (Viton) tubing employed has passed all resistance tests up to 1000 kGy in contact with nitric acid. The connections between the Viton (6 mm outside and 4 mm inner diameters) tubing and the stainless steel coil are composed of an outlet valve with a screw cap of stainless steel.

To know the effective dose rate provided by ^{60}Co sources in static conditions, a Fricke dosimetry measurement [43] using a stainless steel shield with the same thickness of the coil reactor was undertaken, resulting in a dose rate of 35.11 kGy/h. The volume employed for each phase was 130 mL. The flow rate was adjusted to maintain the volume ratio (in the range of 0.31 L/h). As the residence time of solvent within the irradiator coil is only a fraction of the total, the effective dose rate submitted over the coil was determined by taking into account the coil volume, phase residence time and the effective dose through the steel, giving a result of 2.89 kGy/h. Samples of both phases were taken at different absorbed doses during the test loop.

Using the loop designed and shown in Fig. 3, the two main biphasic system of EURO-GANEX process, i.e. An + Ln co-extraction (1) and TRU stripping (2), were irradiated in two different steps: 1) 0.2 mol/L TODGA and 0.5 mol/L DMDOHEMA in OK in contact with 5 mol/L HNO$_3$ irradiated up to 500 kGy; 2) The irradiated organic phase from step 1 was again irradiated up to 40 kGy in contact with an aqueous phase of 0.018 mol/L SO$_3$-Ph-BTP in 0.5 mol/L HNO$_3$, providing a total dose delivered to the organic phase of 540 kGy and just 40 kGy to the stripping aqueous phase. During the irradiation process, neither CDTA nor AHA were included in the experiments.

2.3. Solvent extraction performance

The behavior of the EURO-GANEX process after the two different steps mentioned before (see scheme in Fig. 2) was assessed with spiked samples (^{241}Am and ^{152}Eu) and the phases shown in Table 1.

Samples of the organic phase taken at 200 and 500 kGy after the first irradiation (An + Ln co-extraction), were put in contact with a fresh aqueous phase consisting of 10 %$_{vol}$ of a simulated HAR solution and 0.055 mol/L CDTA in 5 mol/L HNO$_3$ and spiked with 10 μL of ^{241}Am and ^{152}Eu (100 kBq/ml each). The composition of the HAR solution is shown in Table 2 and corresponds to a high-level waste

solution coming from a UOX fuel reprocessing, with an initial ^{235}U enrichment of 3.5%, thermal burn-up of 33 GWd/t$_{HM}$ and 3 years of cooling [36]. The loaded organic phase was twice contacted with an equal volume of fresh 0.5 mol/L HNO$_3$ for 5 min for the scrubbing step.

After the second step of irradiation (TRU stripping step), the behavior of the system was assessed by using samples taken from both irradiated phases (Table 1): TODGA and DMDOHEMA (up to 540 kGy) and 0.018 mol/L SO$_3$-Ph-BTP in 0.5 mol/L HNO$_3$ (from 10 to 40 kGy) and then spiked with 10 μL of ^{241}Am and ^{152}Eu (100 kBq/ ml each). AHA is not included in the extraction experiments because neither Pu and Np were used in the current tests.

All extraction experiments were performed by mixing 500 μL of both, aqueous and organic phases, for 30 min at room temperature (22 ± 2 °C). Then, the phases were separated by centrifugation (5 min at 5000 rpm) and aliquots of each were taken for analysis (300 μL for gamma and 100 μL ICP-MS).

For high energy gamma spectroscopy measurements, a High Purity−Germanium detector with an intrinsic efficiency of 20% was used, using Genie-2000 (Canberra) as analysis software. The gamma characteristic photopeaks at 59.5 keV and 121.8 keV were analyzed for ^{241}Am and ^{152}Eu, respectively.

The concentration of the elements presented in the HAR solution as well as those coming from the stainless steel corrosion products (Fe, Cr, Ni and Mo) were determined by ICP-MS. The organic and aqueous phases were analyzed directly after a suitable dilution in HNO$_3$ (2−5.%). All extraction results are reported as distribution ratio D ($D_M = [M]_{org}/[M]_{aq}$), where D_M between 0.01 and 100 exhibit a maximum error of ±5%. The limit of detection (LOD) for ^{241}Am and ^{152}Eu is 2 and 6 Bq/L, respectively, and for Fe, Cr, Ni and Mo is $2.8 \cdot 10^{-6}$ mmol/L, $5 \cdot 10^{-7}$ mmol/L, $7 \cdot 10^{-7}$ mmol/L and $7 \cdot 10^{-8}$ mmol/L, respectively, based on the dilutions carried out.

2.4. Solvent composition analysis

The chemical composition of the irradiated organic and aqueous samples was determined by HPLC-MS and Raman spectroscopy, respectively. HPLC-MS measurements were performed using an HPLC-MS Bruker EVOQ™ (Triple Quadrupole detector) with a ACE 3 C18-PFP column (50 mm × 2.1 mm) at 40 °C, using a gradient of mobile phase [(A: 0.1% HCOOH in H$_2$O), (B: 0.1% HCOOH in CH$_3$CN)]. APCI$^+$ ionization mode was used for TODGA and DMDOHEMA

Table 1
Composition of the organic and aqueous phases in the different steps of the irradiation test loop and the following extraction experiments.

Experiments step		Solvent formulation	
		Organic phase	Aqueous phase
An + Ln co-extraction	a) Irradiation	**Fresh EURO-GANEX solvent** 0.2 mol/L TODGA + 0.5 mol/L DMDOHEMA in OK	**Fresh** 5 mol/L HNO$_3$
	b) Extraction after the 1st irradiation	**Irradiated EURO-GANEX solvent 200 and 500 kGy** TODGA + DMDOHEMA in OK	**Fresh** 0.055 mol/L CDTA + 10 %$_{vol}$ HAR in 5 mol/L HNO$_3$
Scrubbing	Intermediate step between irradiations	**Irradiated EURO-GANEX solvent from the previous step (500 kGy)** TODGA + DMDOHEMA in OK	**Fresh** in 0.5 mol/L HNO$_3$
TRU stripping	a) Irradiation	**Irradiated EURO-GANEX solvent from the previous step (500 kGy) + scrubbing** TODGA + DMDOHEMA in OK	**Fresh** 0.018 mol/L SO$_3$-Ph-BTP in 0.5 mol/L HNO$_3$
	b) Extraction after the 2nd irradiation	**Irradiated EURO-GANEX solvent from the second step (540 kGy)** TODGA + DMDOHEMA in OK	**Irradiated Aq. phase (10, 20, 30 and 40 kGy)** 0.018 mol/L SO$_3$-Ph-BTP in 0.5 mol/L HNO$_3$

I. Sánchez-García, H. Galán, A. Núñez et al.

Table 2
Composition of the synthetic high active raffinate (HAR) solution listing elements dissolved in 4 mol/L HNO_3 (33 GWd/t_{HM}, Initial enrichment 3.5% ^{235}U) [36].

Lanthanides		Fission/corrosion products	
Elements	mg/L	Elements	mg/L
Ce	463	Ba	280
Eu	35	Cd	18
Gd	35	Cr	100
La	278	Cu	25
Nd	718	Mo	720
Pr	293	Ni	47.5
Sm	140	Pd	198
Y	108	Rb	68
–	–	Rh	73
–	–	Ru	408
–	–	Sn	10
–	–	Sr	180
–	–	Zr	958

quantification, meanwhile ESI$^+$ mode was used for TODGA DCs quantification. The quantification of DMDOHEMA DCs was not carried out due to the absence of the DCs isolated as standards. Samples for HPLC-MS studies were analyzed without pre-evaporation and diluted 1:30,000 in HPLC grade MeOH. Calibration curves were performed for TODGA, DMDOHEMA and each TODGA DCs, from 10 to 1000 ppb, and the correlation coefficients in all cases were in the range of 0.993−0.999. All measurements were performed in triplicate in order to have uncertainty analysis where results show a maximum error of ±3%.

The concentration of SO_3-Ph-BTP was measured by Quantitative Raman Spectroscopy (QRS) using the methodology developed in our previous work [38]. Raman spectra of samples were acquired by using a B&W Tek i-Raman™, model BWS415-785S. A red laser of HeNe with a wavelength of 785 nm with an operating power of 300 mW was used. The spectral range available to this spectrometer is from 175 to 3200 cm^{-1}, with a spectral resolution of ~5 cm^{-1}.

The proton concentration in the aqueous phases was determined potentiometrically by acid-base titration with KOH using an automatic titrator (Metrohm 798 MPT titrino) with an Unitrode as electrode purchased from Metrohm. A dynamic equivalence point of titration was employed for the determination, where the KOH was added in variable volume steps. The electrode was calibrated employing buffer solutions of pH 4.00 and 7.00 supplied by Metrohm.

3. Results and discussion

With the aim of developing a loop that bridges the gap between fundamental studies and sophisticated irradiation loop platforms, the requirements gleaned from static studies have been adapted to a new loop design at the Náyade facility. Hence, the performance and effects of realistic dynamic irradiation during the two main steps of EURO-GANEX, the An + Ln co-extraction and the TRU stripping, are the objects of this study (the compositions employed are summarised in Table 1 and Fig. 2).

The An + Ln co-extraction system (0.2 mol/L TODGA + 0.5 mol/L DMDOHEMA in OK in contact with 5 mol/L HNO_3) was irradiated at 200 and 500 kGy, simulating an accumulated absorbed dose of the recycled organic phase [44] that also allows a direct comparison to previous results, albeit without any form of solvent cleaning or bleeding that would likely be present on an actual operational plant. CDTA was not included in the aqueous phase since the expected dose in any one single pass for the aqueous phase is much lower than 500 kGy, and the irradiation of both phases together would not reproduce a realistic situation. During the irradiation

process, a color change of the organic phase from slightly yellow to dark yellow was found, but no third phase formation, precipitate, or other physical changes were observed, as expected from previous results.

After the An + Ln co-extraction irradiation step, the 5 mol/L HNO_3 aqueous phase was replaced by a fresh solution containing CDTA, a 10 %$_{vol}$ of HAR solution (composition in Table 2) in 5 mol/L HNO_3 and spiked with ^{241}Am and ^{152}Eu. CDTA was now added to evaluate Zr and Pd retention in the aqueous phases since it is already known that some TODGA DCs are also able to extract these metals [11].

A normal phase separation behavior was also obtained without any precipitates or third phase formation. The variation of $D_{Am(III)}$ and $D_{Eu(III)}$ as a function of absorbed dose is shown in Fig. 4. As expected from static studies, both metals are well extracted into the organic phase even after 500 kGy of absorbed dose (D > 100), although a slight decrease in the D values is always observed for both elements. Therefore, under the irradiation loop condition applied, the system can still extract An and Ln even after 500 kGy of absorbed dose, corroborating all previous works based on TODGA-based solvents [18,36].

FPs and Ln element concentrations were measured in both phases by ICP-MS, and the distribution ratios of these elements are
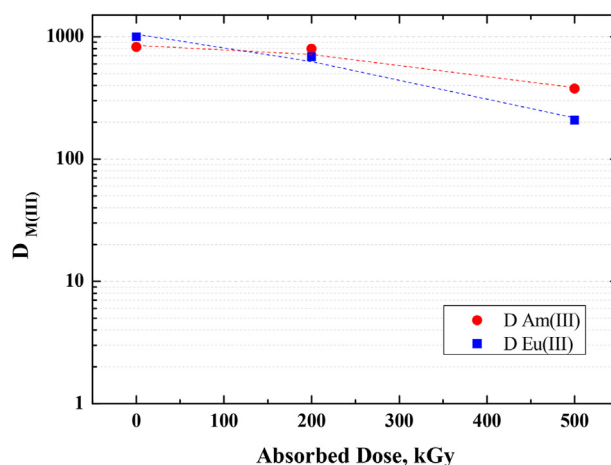

Fig. 4. Distribution ratios of Am(III) and Eu(III) as a function of absorbed dose after the first step of the irradiation loop test (An + Ln co-extraction, see Fig. 2). Org. phase: Irradiated 0.2 mol/L TODGA and 0.5 mol/L DMDOHEMA in OK. Aq. phase: Fresh 0.055 mol/L CDTA + 10 %$_{vol}$ of HAR solution in 5 mol/L HNO_3 spiked with ^{241}Am and ^{152}Eu.

Table 3

Distribution ratios for Ln and FP by fresh and irradiated EURO-GANEX solvent (0.2 mol/L TODGA + 0.5 mol/L DMDOHEMA in OK) at 200 kGy and 500 kGy from a fresh aqueous phase consisting of 5 mol/L HNO_3 with and without 0.055 mol/L CDTA. All aqueous phases contain 10%$_{vol}$ HAR solution. (Note: Mo was not included due to its not-satisfactory measurement in HAR solution).

Element	Extraction			
	0 kGy without CDTA	0 kGy with CDTA	200 kGy with CDTA	500 kGy with CDTA
Cu	0.13	0.12	0.13	0.07
Sr	1.11	1.31	0.62	0.46
Ru	0.19	0.17	0.17	0.21
Cd	0.22	0.22	0.18	0.14
Ba	0.06	0.01	0.02	0.02
Cr, Rb, Rh	<0.01			
Ni	0.02	<0.01	<0.01	<0.01
Zr	> **100**	<0.01	<0.01	<0.01
Pd	> **100**	<0.01	<0.01	<0.01
Y	76.86	62.38	86.55	>100
Ln (La, Ce, Pr, Nd, Sm, Eu, Gd)	>100			

represented as a function of absorbed dose in Table 3. As can be observed, the extraction behavior for most of these elements remains unchanged when the irradiated and non-irradiated samples are compared, showing Y and Ln have high D values in all cases (D > 100). The influence of the CDTA presence on the extraction of Zr and Pd is clearly observed with a significant decrease of the D_{Pd} and D_{Zr} reaching values of D < 0.01, in agreement with previous studies [22,29,45], and this performance is not modified even if the system is irradiated up to 500 kGy.

As the reactor coil employed in the irradiation loop is made of 316 stainless steel, the possible corrosion products as a consequence of the contact with nitric acid and radiation have also been measured by ICP-MS, concluding that Fe, Cr, Ni and Mo are the most relevant stainless steel corrosion products. Fig. 5 shows the evolution of their concentration in the organic and aqueous phases along the first irradiation step (Ln + An co-extraction). The concentration of all corrosion metals measured increases as a function of absorbed dose with Fe, Cr and Ni being the most abundant. Fe was predominantly extracted into the organic phase with 2.54 mmol/L at 500 kGy, albeit there is 0.34 mmol/L in the aqueous phase at the same absorbed dose. This is in agreement with Carrott et al. [45], who explained that DMDOHEMA is responsible for Fe extraction, although TODGA and DMDOHEMA DCs could also account for some of this behaviour. Cr and Ni were kept in the aqueous phase reaching a concentration of 0.54 mmol/L and 0.31 mmol/L, respectively, at the highest absorbed dose (500 kGy). This behaviour is similar to that observed by Peterman et al. [18], who reported ~0.30 mmol/L and ~0.36 mmol/L for Cr and Ni after ~550 kGy, respectively. Mo was found in concentrations lower than ~0.01 mmol/L in both phases.

As previously discussed, after the extraction and before the stripping step, it was necessary to introduce a scrubbing step with a diluted nitric acid (0.5 mol/L) (Fig. 2). Fig. 5 also shows the remaining concentration of corrosion products in the organic phase after this 2nd scrubbing stage. The effectiveness of the scrubbing section to remove mainly Fe and Ni from the organic phase is observed, but not Cr and Mo, which remained in the organic phase, albeit in low concentration.

The acid concentration of the aqueous phase along the steps studied was also checked. The proton concentration decreased from 4.65 mol/L for unirradiated HNO_3 to 3.78 mol/L for the irradiated solution at 500 kGy during the An + Ln co-extraction step. After the first scrubbing stage, the proton concentration was 0.89 mol/L, reaching 0.5 mol/L in the aqueous phase after the second scrubbing stage, which ensured the correct acidity in the organic phase for the next TRU stripping step.

After simulating a long-term used organic phase (after 500 kGy), and the corresponding scrubbing steps, the organic phase was

again irradiated in contact with a new aqueous phase, consisting of 0.018 mol/L SO_3-Ph-BTP in 0.5 mol/L HNO_3, to simulate the possible effects over the global system during the TRU stripping (see Fig. 2). This system was irradiated up to 10, 20, 30 and 40 kGy. AHA hydrolysis in acid media affects the original extraction properties of the system due to its reduction in concentration, but because it also causes a significative reduction in proton concentration due to the formation of NH_3OHNO_3. We have recently published the kinetic study of AHA hydrolysis for these particular conditions and the effects on Ln extraction by a TODGA solvent [39]. In that study, it was demonstrated that for all those studies involving AHA in acid media, the $D_{Ln(III)}$ values after 24 h are negatively affected due to AHA hydrolysis. Therefore, considering that the irradiation takes longer (~8 days) than AHA hydrolysis reactions, to evaluate the radiolytic effects over the extraction performance (D_M values), AHA was not included during the irradiation experiment.

Over the course of the second irradiation step, the aqueous phase containing the SO_3-Ph-BTP darkened considerably, from the green of the unirradiated samples to opaque black of the irradiated samples, which has been widely related to its radiolytic degradation (Fig. 6) [18,23,37,38].

The $D_{Am(III)}$, $D_{Eu(III)}$ and $SF_{Am(III)/Eu(III)}$ values determined at the corresponding doses selected along the irradiation of the TRU stripping step are presented in Fig. 7. In this case, an increasing effect of radiolytic degradation as a function of the dose can be observed just after the first irradiation step (10 kGy), where the $D_{Am(III)}$ increases reaching values higher than 1 and indicating that Am is not effectively stripped into the aqueous phase. This means
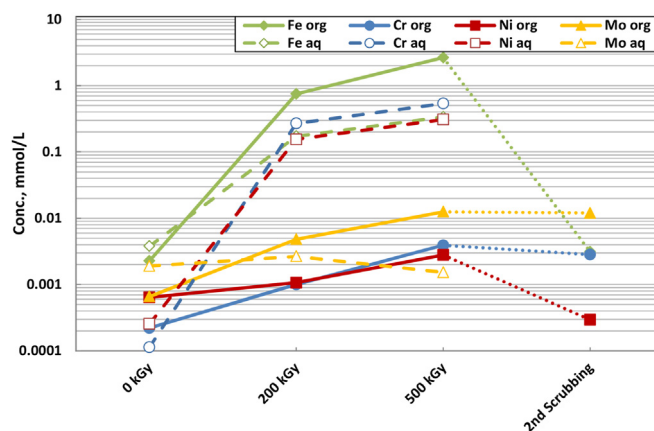

Fig. 5. Evolution of the concentration of stainless steel corrosion products Fe, Cr, Ni and Mo during An + Ln co-extraction and scrubbing steps of EURO-GANEX irradiation loop.
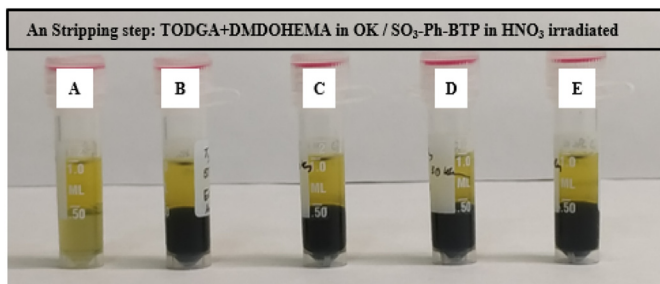
Fig. 6. TRU stripping samples after different absorbed doses. Org. phase: 0.2 mol/L TODGA and 0.5 mol/L DMDOHEMA in OK irradiated at 540 kGy. Aq. phase: 0.018 mol/L SO$_3$-Ph-BTP in 0.5 mol/L HNO$_3$ irradiated at different doses: (A) 0 kGy, (B) 10 kGy, (C) 20 kGy, (D) 30 kGy and (E) 40 kGy.
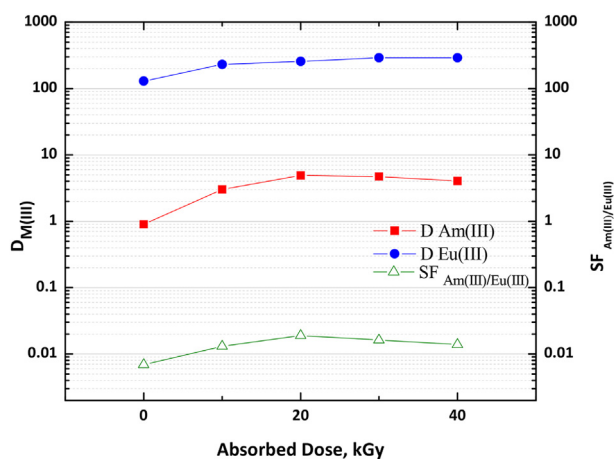

Fig. 7. Distribution ratios of Am(III) and Eu(III) as a function of dose for the second irradiation step (TRU stripping, see Fig. 2). Org. phase: Irradiated 0.2 mol/L TODGA and 0.5 mol/L DMDOHEMA in OK at 540 kGy, Aq. phase: 0.018 mol/L SO$_3$-Ph-BTP in 0.5 mol/L HNO$_3$ irradiated at different doses (from 0 to 40 kGy).

that the system would lose the ability to separate An from Ln just after a few kGy, in disagreement with previous studies where both phases have been irradiated together and maintained the An and Ln separation up to 50 kGy, in static conditions [38], or up to 174 kGy in a loop test [18]. However, it is important to note that both D values increase from the first irradiation point, with the D$_{Am(III)}$ value at 0 kGy being close to 1, giving place to an inadequate stripping of americium into the aqueous phase by the SO$_3$-Ph-BTP even in the absence of radiation. This result at 0 kGy is in disagreement with previous studies where the EURO-GANEX system was assessed giving a D$_{Am(III)}$ < 0.1 [45]. For that reason, these results at 0 kGy may not be related to the radiolytic degradation of SO$_3$-Ph-BTP, but also to other effects coming from the organic phase such as pH variations, presence of corrosion metals or compositional variations. However, when SO$_3$-Ph-BTP is irradiated, the degradation itself and the subsequent formation of its DCs produces effects to consider other than just the D$_{Am(III)}$ values increase. Therefore, understanding the effect of radiation and DCs on this change in D$_{Am(III)}$ will require further work.

The remaining concentration of corrosion metals coming from the organic phase will be added to those from the corrosions due to the new irradiation step (containing SO$_3$-Ph-BTP) during the TRU stripping step irradiation. Fig. 8 shows the evolution of their concentrations in the organic and aqueous phases under irradiation during the TRU stripping step. As can be observed, the low doses applied did not produce a significant increase in corrosion metal concentration compared to the previous irradiation step. Contrary

to the previous step, now Fe was found mostly in the aqueous phase, in agreement with the previous study carried out by Carrott et al. [45] where they reported that Fe is not extracted at low acid concentrations (up to 1 mol/L HNO$_3$) by the EURO-GANEX solvent. Cr and Ni were also found mainly in the aqueous phase, however, Mo was kept principally in the organic phase albeit at a low concentration (0.01 mmol/L).

The presence of corrosion metals during the TRU stripping could cause the unexpected D$_{M(III)}$ values shown in Fig. 7. Therefore, additional extraction experiments with the EURO-GANEX solvent to check the TRU stripping as a function of the Fe, Cr and Ni initial concentrations in the aqueous phase have been carried out and the results are summarised in Table 4. These initial metal concentrations were selected as a result of the corrosion experiments (see Fig. 8). As the concentration of Fe, Cr and Ni increases (Exp. 2−5, Table 4), the D$_{Am(III)}$ values also increase. These results show that Fe, Cr and Ni are complexed by SO$_3$-Ph-BTP and could compete with Am, thus decreasing its complexation. Hence, the presence of these metals in the aqueous phase effectively influences the extraction capacity of the system, modifying the distribution ratios and therefore, the system performance. It should also be noted that aqueous solutions of these experiments darkened, especially when a high Fe concentration was added (Exp. 4 and 5, Table 4), similar to the irradiated TRU stripping solution obtained in the irradiation test loop. This result highlights that the color change in the SO$_3$-Ph-BTP solution during the irradiation process could not only be attributed to its radiolytic degradation, but also the presence of metals such as Fe.

As in previous steps, the acid concentration of the aqueous phase during the TRU step was also checked and it is summarised in Table 5. The proton concentration increases from approximately 0.50 mol/L when SO$_3$-Ph-BTP is unirradiated, to 0.84 mol/L for all the absorbed doses studied. This significant increase in the acidity could be one of the reasons for the unexpectedly high D$_{Am(III)}$ values observed in Fig. 7. This increase is still unexplained since it could be due to the ineffective adjustment of the conditions after the first irradiation step or unexpectedly high degradation of the aqueous phase.

Otherwise, the changes observed in the composition caused by the degradation of extractants also affect the extraction capacity of the system. Therefore, although distribution ratios give us a lot of information about the systems and allow the prediction of their behavior, they should not be used as the only metric for ligand degradation. Hence, to have a global picture of what is happening and a more complete understanding, the composition of both the organic and the aqueous phases of the corresponding An + Ln co-
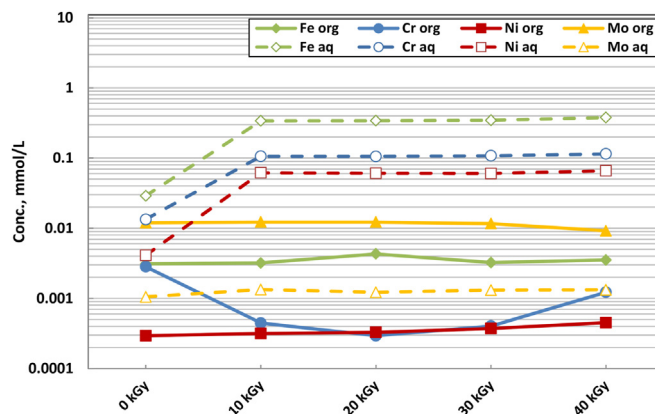

Fig. 8. Evolution of the concentration of stainless steel corrosion products Fe, Cr, Ni and Mo during TRU stripping step of EURO-GANEX irradiation loop.

Table 4

Distribution ratios of An(III) and Ln(III) by fresh EURO-GANEX solvent (0.2 mol/L TODGA + 0.5 mol/L DMDOHEMA in OK) from the fresh aqueous phase consisting of 0.018 mol/L SO_3-Ph-BTP varying the Fe(III), Cr(III) and Ni(II) initial concentrations in the aqueous phase.

Exp.	Samples composition					Distribution ratios	
	Org. phase	Aq. phase					
		Composition	$Fe(III)_{in}$, mmol/L	$Cr(III)_{in}$, mmol/L	$Ni(III)_{in}$, mmol/L	$D_{Am(III)}$	$D_{Eu(III)}$
1	0.2 mol/L TODGA +	0.018 mol/L SO_3-Ph-BTP in 0.5 mol/L HNO_3	–	–	–	0.09	22.5
2	0.5 mol/L DMDOHEMA in OK		–	0.02	0.02	0.18	35.4
3			–	0.10	0.09	0.21	55.4
4			0.02	0.02	0.02	0.30	65.9
5			0.36	0.10	0.09	0.31	41.0

Table 5

Proton concentration monitoring for all aqueous samples involved during the TRU stripping step of EURO-GANEX process.

EURO-GANEX process step	Aqueous phase sample	Absorbed Dose, kGy	$[H^+]$, mol/L
TRU Stripping	0.018 mol/L SO_3-Ph-BTP in 0.5 mol/L HNO_3	0	0.48
		10	0.81
		20	0.80
		30	0.79
		40	0.84

extraction and TRU stripping steps were investigated. The composition of the organic phase has been analyzed qualitatively and quantitatively by HPLC-MS, while the composition of the aqueous phase was analyzed by Raman spectroscopy, using the methodology presented in our recent works [23,24,38].

First, the effect over the main extractants in the organic phase was analyzed. Fig. 9 shows the TODGA and DMDOHEMA concentrations remaining after both steps of the irradiation loop, An + Ln co-extraction and TRU stripping steps (up to 500 and 540 kGy, respectively). As expected, the extractants concentrations diminish as a function of dose, reaching a decrease of 32% for TODGA (25% after An + Ln co-extraction and an additional 7% after TRU stripping) and 33% for DMDOHEMA (25% after An + Ln co-extraction and additional 8% after TRU stripping).

After the first step, on the one hand, the results related to TODGA agree with those obtained by Peterman et al. [18] during its irradiation loop, where a decrease of TODGA concentration of ~37% at 540 kGy in dynamic conditions was reported. In addition, the behavior observed for DMDOHEMA is also in agreement with the results published by Berthon et al. [46] where an ~37% malonamide

Fig. 9. TODGA and DMDOHEMA concentration as a function of the absorbed dose. Fresh EURO-GANEX solvent (reference sample), irradiated at 200 and 500 kGy in contact with of 5 mol/L HNO_3, and irradiated at 500 kGy in contact with 5 mol/L HNO_3 and extra 40 kGy with 0.018 mol/L SO_3-Ph-BTP in 0.5 mol/L HNO_3.

concentration decrease is observed when 0.65 mol/L DMDOHEMA in dodecane is irradiated in contact with 3 mol/L HNO_3 in static conditions. If we compare the current results with our previous studies where TODGA/SO_3-Ph-BTP systems were irradiated in static contact up to 500 kGy, a higher resistance of the organic solvent can now be observed. In that previous works [23,24], more than a 50% decrease in TODGA concentration under different air, air sparging and Ar atmospheres was found, indistinctly if SO_3-Ph-BTP was present in the aqueous phase. This higher resistance could be explained because of the different nitric acid concentration of the aqueous phase in contact, but also, because of the high content of DMDOHEMA in the current experiment. According to the dose constant described for TODGA and DMDOHEMA in dodecane [47], statistically, TODGA preferentially reacts with the n-dodecane radical cation. However, the relatively magnitude of the electron fraction of DMDOHEMA coupled with the decreases of the diluent acts to decrease the magnitude of TODGA degradation.

Although the irradiation of sytems involved in the TRU stripping step only adds a few additional kGy, the degradation of the organic solvent is proportionally much higher than expected, increasing by 7 and 8% for TODGA and DMDOHEMA, respectively, after only 40 kGy, compared to the 25% concentration decrease observed after the 500 kGy applied during the first step of irradiation. This proportionally higher degradation could be attributed to the presence of SO_3-Ph-BTP and/or a lower acidity of the aqueous phase (and therefore decrease in nitrate concentrations in each phase).

In parallel to the main extractants, TODGA and DMDOHEMA DCs were identified. Fig. 10 shows the qualitative HPLC-MS analysis of the reference and irradiated samples after the An + Ln co-extraction and TRU stripping of the irradiation test loop (200, 500 and 540 kGy, respectively), where eight of the main typical TODGA DCs [10,12,34,35] and six of the DMDOHEMA DCs [28,46] can be identified, and which structures are shown in Fig. 11A and Fig. 11B, respectively. Moreover, three new signals (shown as stars in Fig. 10) have been identified as possible undescribed DCs (m/z = 383.3, r.t = 7.10 min, possible chemical formula $[C_{22}H_{42}N_2O_3+H]^+$; m/z = 400.2, r.t = 7.75 min, possible chemical formula $[C_{23}H_{45}NO_4+H]^+$; and m/z = 498.3, r.t = 11.55 min, possible chemical formulas $[C_{28}H_{51}NO_6+H]^+$ or $[C_{29}H_{56}NO_5+H]^+$; some of the possible hypothetical DCs structures matching with new signals are shown in Fig. 11C). The formation of these new possible DCs could be attributed to better
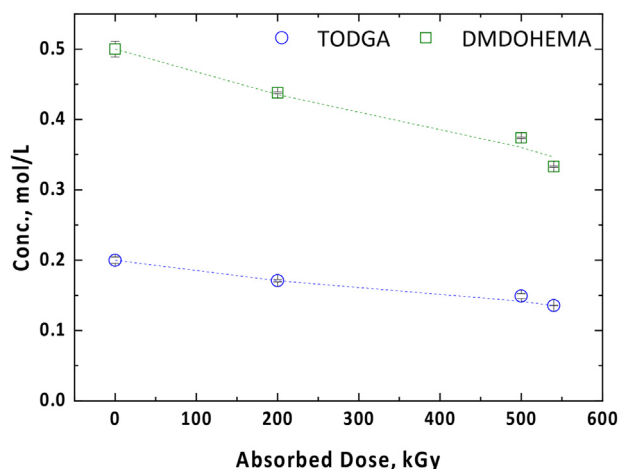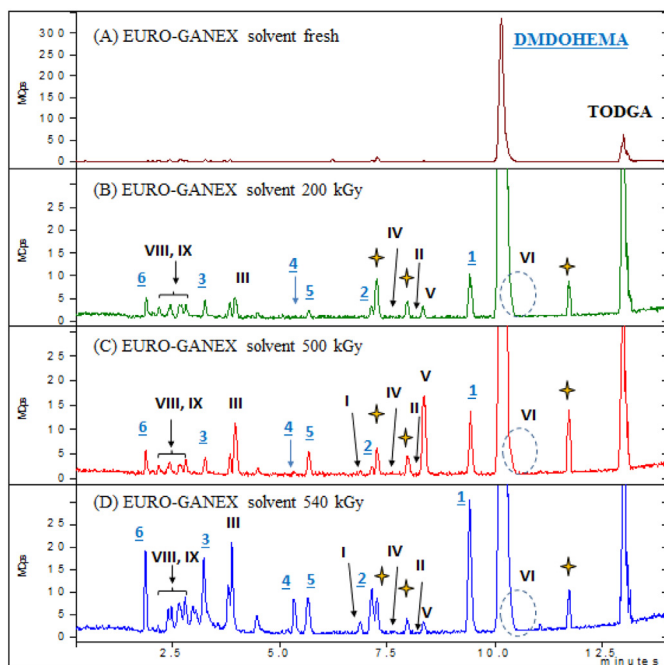
I. Sánchez-García, H. Galán, A. Núñez et al.

Fig. 10. Qualitative HPLC-MS chromatograms of EURO-GANEX solvents obtained along the irradiation test loop: (A) fresh or reference sample, and irradiated in contact with 5 mol/L HNO$_3$ at (B) 200 kGy; (C) 500 kGy; (D) 500 kGy and other 40 kGy in contact with 0.018 mol/L SO$_3$-Ph-BTP in 0.5 mol/L HNO$_3$. (Note: Since TODGA DC VI appears at the same time as DMDOHEMA, the signal is overlapped and therefore it is shown in that way.)

Fig. 11. Structures of (A) TODGA and (B) DMDOHEMA with their respectives DCs, and (C) Hypothetical structures for the new signals found by HPLC-MS.
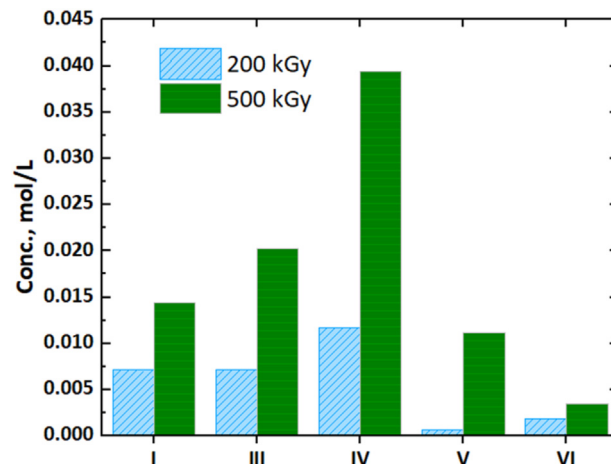

Fig. 12. HPLC-MS quantitative analysis of different TODGA DCs when EURO-GANEX solvent is irradiated in the irradiation test loop with 5 mol/L HNO$_3$ at 200 and 500 kGy in the An + Ln co-extraction step.

contact between phases and a higher oxygen content during the irradiation process as a consequence of the dynamic conditions. The appearance of new peaks is in agreement with our recent works [23,24], where the presence of new hypothetical TODGA DCs was reported when the irradiation occurs in static conditions but with a higher oxygen content using an air sparging flow.

The quantification of TODGA DCs was carried out, whereas for the DCs of DMDOHEMA it was not possible due to the unavailability of isolated products in order to create calibration curves. Fig. 12 shows the quantification of TODGA DCs: I, III, IV, V and VI by HPLC-MS for samples irradiated at 200 kGy and 500 kGy. The other DCs are not shown because their concentrations were lower than the LOD. An increase of all DCs concentrations as a function of the absorbed dose in our studied conditions can be observed, as a consequence of TODGA degradation. Typically the DCs IV, V and VI are the most abundant due to the radiation effect over the weakest bonds of TODGA (C-O$_{ether}$ and N-C) [34,35]. However, from the results observed in Fig. 12, it can be seen that under the current irradiation test loop conditions, the proportion of the main DCs changes, with I, III and IV being the majority. These results are also in agreement with our previous work, where the TODGA-based solvent in contact with nitric acid was irradiated using an air sparging flow [23,24]. One of the conclusions of that study was that a higher oxygen content or better mixing between phases favored the degradation pathway to form I and III over V and VI. The current similar results could corroborate that hypothesis. Therefore, the high presence of the DCs and their possible accumulation during the process should be considered for the development of the clean-up strategies for the EURO-GANEX process.

The radiolytic degradation of SO$_3$-Ph-BTP was also analyzed by QRS. The spectra of the irradiated samples, fitted curves and calibration curves are shown in Appendix A of the ESI. Fig. 13 shows the SO$_3$-Ph-BTP concentration decreases as a function of absorbed dose, i.e., approx. 65% is lost at 40 kGy. This degradation seems higher than that observed in the literature (see Table 6), but the quantification of this molecule has given place to controversial results. As Table 6 clearly shows the extent of degradation can vary from 0 to 65% over 40−200 kGy. The main appreciable differences in all of these studies are the method of irradiation and the method of measurement. The work presented here uses a dynamic irradiation as expected on plants and a direct quantification of the molecular backbone, therefore, these results could offer greater insight to the effect of radiation on extraction systems containing SO$_3$-Ph-
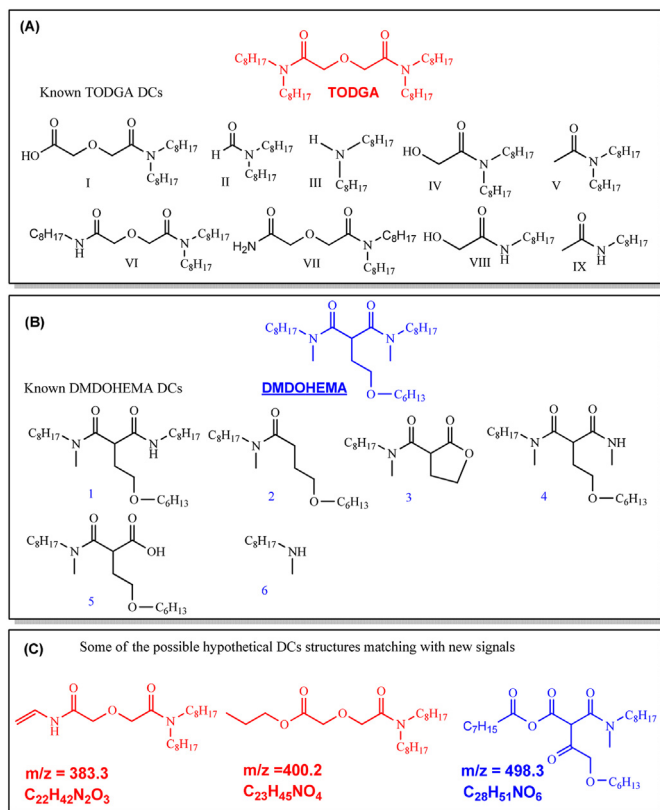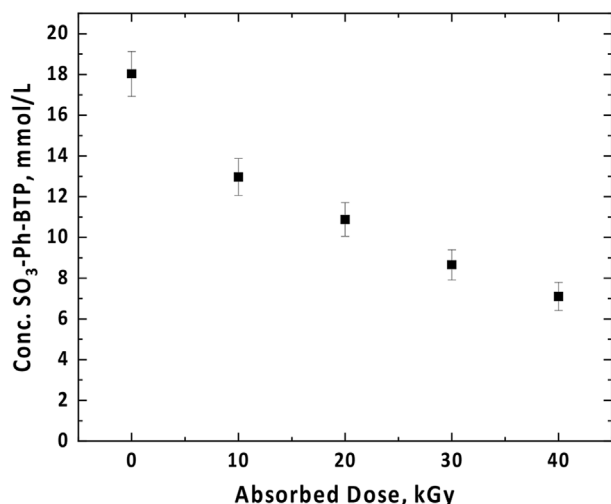
Fig. 13. SO$_3$-Ph-BTP concentration obtained by Raman spectroscopy as a function of absorbed dose for the irradiation test loop of the TRU stripping step.

BTP. From the results obtained in this experiment, the SO$_3$-Ph-BTP degradation follows a kinetic law of order 1 with respect to the pyridine concentration. This kinetic degradation constant k' has been calculated to be 0.023 kGy^{-1}. This result of SO$_3$-Ph-BTP degradation obtained during the current design test loop demonstrates that this compound is very susceptible to degradation under the studied radiation conditions, in agreement with the studies found in the literature [23,37,38,48], and highlights the importance of fitting the experimental conditions during the experiment where, in this case, the degradation observed is slightly higher than previous studies.

4. Conclusions

In this work, an irradiation test loop has been developed for the first time that combines the advantages of simple static irradiation experiments with those of sophisticated irradiation dynamic plants, providing an easy modification of settings with a really low volume requirement. This new design allows the simulation of process relevant conditions such as the composition of phases, the contact between phases involved, the oxygen content and the dose expected for each phase. This new irradiation loop implemented at the Náyade irradiation facility at CIEMAT has been initially

developed for assessing the performance of the two main steps of the EURO-GANEX process (An + Ln co-extraction and TRU stripping), under the most relevant and realistic experimental conditions in an easy and adaptable way.

The first step of the loop simulates a long-term irradiation (500 kGy) of the EURO-GANEX solvent in contact with a high nitric acid concentration, which corresponds to many consecutive cycles of An and Ln co-extraction, maintaining an excellent extraction performance for An and Ln. The monitoring during the first irradiation step of the different effects of gamma radiation over the system (stainless steel corrosion, acidity, ligand concentration and presence of degradation compounds) still revealed a situation which should work in a process. Fortunately, the scrubbing section introduced between the first and second irradiation steps of the loop was effective in reducing the proton concentration and removing some of the corrosion metals extracted into the organic phase that were produced during the irradiation of the system (with the SS test loop). These optimal results have been obtained despite a not insignificant decrease in TODGA and DMDOHEMA concentration and the formation of their degradation compounds. In that sense, small differences between static and dynamic experiments can be highlighted. There was a lower degradation of TODGA and DMDOHEMA in dynamic experiments and small differences in the proportions of the well-known DCs and even the presence of new, as yet unidentified, ones. All of which can be attributed to the greater contact between phases and a higher oxygen content.

The second irradiation step looks to corroborate and extend our stability studies strategy based on TODGA/SO$_3$-Ph-BTP systems, which are highly affected by the experimental conditions chosen, to the TODGA-DMDOHEMA/SO$_3$-Ph-BTP system in dynamic conditions. An unexpected high D$_{Am(III)}$ value was observed from the beginning of the experiment, creating an ineffective separation between An and Ln. This phenomenon could be attributed to the presence of corrosion products, the variation of pH or the ligand degradation.

The additional experiments performed to check a possible role of corrosion metals presence in the Am stripping by SO$_3$-Ph-BTP have revealed a positive correlation between the Fe, Cr and Ni concentrations and the D$_{Am(III)}$ increase. However, the increase reported in the acidity can not be ignored either.

The analysis of the SO$_3$-Ph-BTP concentration showed a progressive decrease as a function of the absorbed dose (obtaining a dose constant (k') of 0.023 kGy^{-1}). Although this result is in agreement with the trend observed for D$_{Am(III)}$ after irradiation, the

Table 6
SO$_3$-Ph-BTP degradation obtained at different conditions (irradiation, concentrations) for different authors by using different methods compared with the one obtained in this work.

Authors	SO$_3$-Ph-BTP degradation	Irradiation condition	Phases composition	Method
Galán et al., 2014 [37]	50%	50 kGy Static Only aq. phase	Org: None; Aq: 10 mmol/L SO$_3$-Ph-BTP in 0.5 mol/L HNO$_3$	Estimated by D$_{Am}$ correlation
Sánchez-Garcia et al., 2020 [38]	50%	50 kGy Static Only aq. phase	Org: None; Aq: 18 mmol/L SO$_3$-Ph-BTP in 0.5 mol/L HNO$_3$	Quantified by QRS
Sánchez-García et al., 2020 [23]	60%	200 kGy Static Two phases	Org: 0.2 mol/L TODGA in OK Aq: 18 mmol/L SO$_3$-Ph-BTP in 0.5 mol/L HNO$_3$	Estimated by D$_{Am}$ correlation
Peterman et al., 2016 [18]	No appreciable degradation	170 kGy Dynamic Two phases	Org: 0.2 mol/L TODGA/5% in 1-Oct/dodecane Aq: 18 mmol/L SO$_3$-Ph-BTP in 0.5 mol/L HNO$_3$	Sulfate quantification by Ion chromatography
This work	65%	40 kGy Dynamic Two phases	Org: 0.2 mol/L TODGA + 0.5 mol/LDMDOHEMA in OK Aq: 18 mmol/L SO$_3$-Ph-BTP in 0.5 mol/L HNO$_3$	Quantified by QRS

unexpected $D_{Am(III)}$ value could be explained as the result of a mixture of factors that can not be isolated, such as pH variations, corrosion metals presence or variations of system composition, but not due to SO_3-Ph-BTP degradation. Further technical adjustment of loop experiments and analysis is still needed to extract final conclusions about TRU stripping step stability. Nevertheless, from these results, it can be stated that after 40 kGy, the remaining concentration of SO_3-Ph-BTP should be enough to preserve an effective separation between An and Ln; although this will also require an exhaustive control of other effects of radiation (pH, DCs, etc.) to ensure an optimal operation during EURO-GANEX process.

Declaration of competing interest

The authors declare that they have no known competing financial interests or personal relationships that could have appeared to influence the work reported in this paper.

Acknowledgements

Appendix A. Supplementary data

Supplementary data to this article can be found online at https://doi.org/10.1016/j.net.2021.11.024.

References

[1] E. Collins, G. DelCul, B. Spencer, R. Jubin, C. Maher, I.-T. Kim, H. Lee, Y.S. Federov, V. Saprykin, V. Beznosyuk, State-of-the-art Report on the Progress of Nuclear Fuel Cycle Chemistry, Organisation for Economic Co-Operation and Development, 2018.

[2] International Atomic Energy Agency, Spent Fuel Reprocessing Options, IAEA-TECDOC-CD-1587, IAEA, Vienna, 2009.

[3] M. Salvatores, Nuclear fuel cycle strategies including partitioning and transmutation, Nucl. Eng. Des. 235 (7) (2005) 805–816.

[4] C. Poinssot, C. Rostaing, S. Greandjean, B. Boullis, Recycling the actinides, the cornerstone of any sustainable nuclear fuel cycles, Procedia Chem. 7 (2012) 349–357.

[5] P. Baron, S. Cornet, E. Collins, G. DeAngelis, G. Del Cul, Y. Fedorov, J. Glatz, V. Ignatiev, T. Inoue, A. Khaperskaya, A review of separation processes proposed for advanced fuel cycles based on technology readiness level assessments, Prog. Nucl. Energy 117 (2019) 103091.

[6] P. Joly, E. Boo, ROADMAP-actinide Separation Processes, Euratom Research and Training Programme on Nuclear Energy, 2015.

[7] S. Bourg, A. Geist, J.M. Adnet, C. Rhodes, B.C. Hanson, Partitioning and transmutation strategy R&D for nuclear spent fuel: the SACSESS and GENIORS projects, EPJ Nucl. Sci. Technol. 6 (2020) 35.

[8] A. Geist, J.M. Adnet, S. Bourg, C. Ekberg, H. Galán, P. Guilbaud, M. Miguirditchian, G. Modolo, C. Rhodes, R. Taylor, An overview of solvent extraction processes developed in Europe for advanced nuclear fuel recycling, part 1-heterogeneous recycling, Separ. Sci. Technol. (2020) 1–16.

[9] INTERNATIONAL ATOMIC ENERGY AGENCY, Assessment of Partitioning Processes for Transmutation of Actinides, 2010. Vienna.

[10] H. Galán, A. Núñez, A.G. Espartero, R. Sedano, A. Durana, J. de Mendoza, Radiolytic stability of TODGA: characterization of degraded samples under different experimental conditions, Procedia Chem. 7 (2012) 195–201.

[11] Núñez, A.; Galán, H.; Cobos, J., TODGA degradation compounds: properties and effects on extraction systems-5400. In GLOBAL 2015 Proceedings..

[12] B.J. Mincher, G. Modolo, S.P. Mezyk, The effects of radiation chemistry on solvent extraction: 1. Conditions in acidic solution and a review of TBP radiolysis, Solvent Extr. Ion Exch. 27 (1) (2009) 1–25.

[13] B.J. Mincher, G. Modolo, S.P. Mezyk, The effects of radiation chemistry on solvent extraction 3: a review of actinide and lanthanide extraction, Solvent Extr. Ion Exch. 27 (5–6) (2009) 579–606.

[14] B.J. Mincher, G. Modolo, S.P. Mezyk, The effects of radiation chemistry on solvent extraction 4: separation of the trivalent actinides and considerations for radiation-resistant solvent systems, Solvent Extr. Ion Exch. 28 (4) (2010)

[15] 415–436.

[15] M.C. Charbonnel, L. Berthon, B. Cames, L. Venault, S. Peuget, In Overview of the French Radiation Chemistry Studies, Radical Behavior Workshop, 2015. Idaho, July 20-22; Idaho.

[16] D.R. Peterman, B.J. Mincher, C.L. Riddle, R.D. Tillotson, Summary Report on Gamma Radiolysis of TBP/n-dodecane in the Presence of Nitric Acid Using the Radiolysis/hydrolysis Test Loop, Idaho National Laboratory (INL), 2010.

[17] M. Miguirditchian, C. Sorel, B. Camès, I. Bisel, P. Baron, D. Espinoux, J. Calor, C. Viallesoubranne, B. Lorrain, M. Masson, In HA demonstration in the Atalante facility of the GANEX 1st cycle for the selective extraction of Uranium from HLW, Proc. GLOBAL (2009) 1032–1036.

[18] D. Peterman, A. Geist, B. Mincher, G. Modolo, M.H. Galán, L. Olson, R. McDowell, Performance of an i-SANEX system based on a water-soluble BTP under continuous irradiation in a γ-radiolysis test loop, Ind. Eng. Chem. Res. 55 (39) (2016) 10427–10435.

[19] D.R. Peterman, L.G. Olson, Summary of ALSEP Test Loop Solvent Irradiation Testing, Idaho National Laboratory.(INL), 2016.

[20] R. Taylor, M. Carrott, H. Galán, A. Geist, X. Hères, C. Maher, C. Mason, R. Malmbeck, M. Miguirditchian, G. Modolo, The EURO-GANEX process: current status of flowsheet development and process safety studies, Procedia Chem. 21 (2016) 524–529.

[21] M. Carrott, K. Bell, J. Brown, A. Geist, C. Gregson, X. Hères, C. Maher, R. Malmbeck, C. Mason, G. Modolo, Development of a new flowsheet for co-separating the transuranic actinides: the "EURO-GANEX" process, Solvent Extr. Ion Exch. 32 (5) (2014) 447–467.

[22] R. Malmbeck, D. Magnusson, S. Bourg, M. Carrott, A. Geist, X. Hérès, M. Miguirditchian, G. Modolo, U. Müllich, C. Sorel, Homogenous recycling of transuranium elements from irradiated fast reactor fuel by the EURO-GANEX solvent extraction process, Radiochim. Acta 107 (9–11) (2019) 917–929.

[23] I. Sánchez-García, H. Galán, J.M. Perlado, J. Cobos, Development of experimental irradiation strategies to evaluate the robustness of TODGA and water-soluble BTP extraction systems for advanced nuclear fuel recycling, Radiat. Phys. Chem. 177 (2020), 109094.

[24] I. Sánchez-García, H. Galán, J.M. Perlado, J. Cobos, Stability studies of GANEX system under different irradiation conditions, EPJ Nucl. Sci. Technol. 5 (2019) 19.

[25] J.-M. Adnet, M. Miguirditchian, C. Hill, X. Heres, M. Lecomte, M. Masson, P. Brossard, P. Baron, In Development of new hydrometallurgical processes for actinide recovery: GANEX concept, Proceedings of Global, Paper no 119 (2005).

[26] Y. Sasaki, Y. Sugo, S. Suzuki, S. Tachimori, The novel extractants, diglycolamides, for the extraction of lanthanides and actinides in HNO₃−n-dodecane system, Solvent Extr. Ion Exch. 19 (1) (2001) 91–103.

[27] S.A. Ansari, P.N. Pathak, V.K. Manchanda, M. Husain, A.K. Prasad, V.S. Parmar, N,N,N′,N′-Tetraoctyl Diglycolamide (TODGA): a promising extractant for actinide-partitioning from high-level waste (HLW), Solvent Extr. Ion Exch. 23 (4) (2005) 463–479.

[28] L. Berthon, J. Morel, N. Zorz, C. Nicol, H. Virelizier, C. Madic, DIAMEX process for minor actinide partitioning: hydrolytic and radiolytic degradations of malonamide extractants, Separ. Sci. Technol. 36 (5–6) (2001) 709–728.

[29] M. Sypula, A. Wilden, C. Schreinemachers, R. Malmbeck, A. Geist, R. Taylor, G. Modolo, Use of polyaminocarboxylic acids as hydrophilic masking agents for fission products in actinide partitioning processes, Solvent Extr. Ion Exch. 30 (7) (2012) 748–764.

[30] A. Geist, U. Müllich, D. Magnusson, P. Kaden, G. Modolo, A. Wilden, T. Zevaco, Actinide (III)/lanthanide (III) separation via selective aqueous complexation of actinides (III) using a hydrophilic 2, 6-bis (1, 2, 4-triazin-3-yl)-pyridine in nitric acid, Solvent Extr. Ion Exch. 30 (5) (2012) 433–444.

[31] R. Taylor, I. May, A. Wallwork, I. Denniss, N. Hill, B.Y. Galkin, B.Y. Zilberman, Y.S. Fedorov, The applications of formo-and aceto-hydroxamic acids in nuclear fuel reprocessing, J. Alloys Compd. 271 (1998) 534–537.

[32] M. Carrott, O. Fox, C. Maher, C. Mason, R.J. Taylor, S.I. Sinkov, G.R. Choppin, Solvent extraction behavior of plutonium (IV) ions in the presence of simple hydroxamic acids, Solvent Extr. Ion Exch. 25 (6) (2007) 723–745.

[33] M. Carrott, C. Gregson, R. Taylor, Neptunium extraction and stability in the GANEX solvent: 0.2 M TODGA/0.5 M DMDOHEMA/kerosene, Solvent Extr. Ion Exch. 31 (5) (2013) 463–482.

[34] Y. Sugo, Y. Sasaki, S. Tachimori, Studies on hydrolysis and radiolysis of N, N, N′, N′-tetraoctyl-3-oxapentane-1, 5-diamide, Radiochim. Acta 90 (3) (2002) 161–165.

[35] C.A. Zarzana, G.S. Groenewold, B.J. Mincher, S.P. Mezyk, A. Wilden, H. Schmidt, G. Modolo, J.F. Wishart, A.R. Cook, A comparison of the γ-radiolysis of TODGA and T (EH) DGA using UHPLC-ESI-MS analysis, Solvent Extr. Ion Exch. 33 (5) (2015) 431–447.

[36] G. Modolo, H. Asp, C. Schreinemachers, H. Vijgen, Development of a TODGA based process for partitioning of actinides from a PUREX raffinate Part I: batch extraction optimization studies and stability tests, Solvent Extr. Ion Exch. 25 (6) (2007) 703–721.

[37] H. Galán, D. Munzel, A. Núñez, U. Müllich, J. Cobos, A. Geist, In Stability and recyclability of SO₃-Ph-BTP for i-SANEX process development, in: Proceedings of the International Solvent Extraction Conference (ISEC 2014), 2014, pp. 137–143.

[38] I. Sánchez-García, L.J. Bonales, H. Galán, J.M. Perlado, J. Cobos, Radiolytic Degradation of sulfonated BTP and acetohydroxamic acid under EURO-GANEX conditions, Radiat. Phys. Chem. 183 (2021), 109402.

[39] I. Sánchez-García, L.J. Bonales, H. Galán, J.M. Perlado, J. Cobos, Spectroscopic study of acetohydroxamic acid (AHA) hydrolysis in the presence of europium. Implications in the extraction system studies for lanthanide and actinide separation, New J. Chem. 43 (39) (2019) 15714—15722.

[40] J. de Mendoza, B. Camafort, A.G. Espartero, A. Núñez, H. Galán, TODGA Industrial Scale-Up Report, ACSEPT FP7-CP-2007-211 267, 2009.

[41] Facility, N. http://fusionwiki.ciemat.es/wiki/LNF:Technology#NAYADE_Co-60_irradiation_facility (accessed October 2020)..

[42] R.A. Leonard, Design principles and applications of centrifugal contactors for solvent extraction, in: Ion Exchange and Solvent Extraction, CRC Press, 2009, pp. 576—629.

[43] H. Fricke, E.J. Hart, The Oxidation of Fe++ to Fe+++ by the irradiation with X-Rays of solutions of ferrous sulfate in sulfuric acid, J. Chem. Phys. 3 (1) (1935) 60—61.

[44] D. Magnusson, B. Christiansen, R. Malmbeck, J.P. Glatz, Investigation of the radiolytic stability of a CyMe4-BTBP based SANEX solvent, Radiochim. Acta 97

[45] M. Carrott, A. Geist, X. Hères, S. Lange, R. Malmbeck, M. Miguirditchian, G. Modolo, A. Wilden, R. Taylor, Distribution of plutonium, americium and interfering fission products between nitric acid and a mixed organic phase of TODGA and DMDOHEMA in kerosene, and implications for the design of the "EURO-GANEX" process, Hydrometallurgy 152 (2015) 139—148.

[46] L. Berthon, S. Journet, V. Lalia, J. Morel, N. Zorz, C. Berthon, B. Amekraz, Use of Chromatographic Techniques to Study a Degraded Solvent for Minor Actinides Partitioning: Qualitative and Quantitative Analysis, CEA VALRHO, 2004.

[47] Y. Sugo, Y. Izumi, Y. Yoshida, S. Nishijima, Y. Sasaki, T. Kimura, T. Sekine, H. Kudo, Influence of diluent on radiolysis of amides in organic solution, Radiat. Phys. Chem. 76 (5) (2007) 794—800.

[48] G.P. Horne, S.P. Mezyk, N. Moulton, J.R. Peller, A. Geist, Time-resolved and steady-state irradiation of hydrophilic sulfonated bis-triazinyl-(bi) pyridines—modelling radiolytic degradation, Dalton Trans. 48 (14) (2019) 4547—4554.

(9) (2009) 497—502.